Competition and water stress indices as predictors of Pinus halepensis Mill. radial growth under drought

Manon Helluy, Bernard Prévosto, Maxime Cailleret, Catherine Fernandez, Philippe Balandier

1 **Competition and water stress indices as predictors of *Pinus halepensis* Mill. radial growth**

2 **under drought**

3 Manon HELLUY[1,2,3]*, Bernard PREVOSTO[1], Maxime CAILLERET[1], Catherine FERNANDEZ[2], Philippe

4 BALANDIER[4]

5

6 [1] Irstea UR RECOVER, 3275 Route de Cézanne, F-13182 Aix-en-Provence, France

7 [2] IMBE, Aix Marseille Université, Avignon Université CNRS, IRD, UMR 7263, 3 place Victor-Hugo, F-13331

8 Marseille cedex 3, France

9

10 [4] Irstea, U.R. Forest Ecosystems, Domaine des Barres, F-45290 Nogent-sur-Vernisson, France

11

12 *corresponding author

13

14 E-mail addresses: manon.helluy@irstea.fr (M. Helluy) ; bernard.prevosto@irstea.fr (B. Prévosto), maxime.cailleret@irstea.fr

15 (M. Cailleret); catherine.fernandez@imbe.fr (C. Fernandez); philippe.balandier@irstea.fr (P. Balandier)

16

17

18

19

20

21

22

23

24

25

26

27

28

29

30 **Declaration of interest: none.**

31 **Abstract**

32   The frequency, duration, and severity of drought events are expected to increase in the Mediterranean

33 area as a result of climate change, with strong impacts on forest ecosystems and in particular individual tree growth.

34 Tree growth response to drought is strongly influenced by local site and stand characteristics that can be quantified

35 using competition indices (CIs) and water stress indices (WSIs). These indices have been widely used to predict

36 tree growth; however, they are numerous, and few studies have investigated them jointly. In this context, we

37 investigated the potential of using CIs and WSIs to investigate tree behaviour under drought. The main objective

38 of this study was to quantify *P. halepensis* Mill. annual radial growth using tree size from the previous year, CIs

39 and WSIs.

40   We studied twelve 50-year-old *Pinus halepensis* plots located in the South-East of France distributed in

41 different density treatments (light, medium and dense). At each plot, all trees were measured (height,

42 circumference), spatialized and the ring-widths were measured for ~15 trees. We also developed a two-strata (over-

43 and understorey) forest water balance model to simulate soil water content at a daily resolution based on stand

44 characteristics (LAI values in particular) and soil properties. A mixed modelling approach was eventually used to

45 investigate the drivers of *P. halepensis* annual radial growth and to test the performance of five CIs and four WSIs.

46   The best growth model included tree size, the sum of Basal Area of Larger trees in a 5m-radius (BAL;

47 as CI), and the number of days that trees experienced water stress in a year (as WSI) as predictors. This model

48 explained up to 56 % of the variance in observed pine tree growth, which increased up to 77% when the individual

49 tree was included as a random effect on the intercept. We found that distance-independent CIs can perform as well

50 as distance-dependent CIs in our study site. The duration of drought alone appeared to better predict tree growth

51 than drought intensity and duration, or drought timing. The selected model led us to reaffirm the positive effect of

52 thinning on tree secondary growth when facing long and intense drought.

53

54

55

56 **Keywords**

57 Radial growth; competition; water stress; *Pinus halepensis;* Mediterranean forests; model

58

59

1. INTRODUCTION

Drought has been identified as the main concern for the current and future functioning of Mediterranean forest ecosystems (Peñuelas *et al.*, 2017). It strongly impacts the physiological functions of Mediterranean tree and shrub species, limiting their annual growth (Barbeta *et al.*, 2015; Borghetti *et al.*, 1998; Gazol et al., 2018; Ogaya *et al.*, 2003). Drought can also induce individual tree mortality and forest dieback in cases of long-term or extreme drought events (Allen *et al.*, 2010; Carnicer *et al.*, 2011; Greenwood *et al.*, 2017; Hayles *et al.*, 2007). Climate models project an increase in temperature – leading to increased potential evapotranspiration – combined with a decrease in precipitation for the Mediterranean area (Giorgi, 2006). This will likely lead to an increase in the duration, intensity and frequency of droughts (Cramer *et al*., 2018). In this context, understanding the processes underlying the response of trees to drought is not only important for fundamental knowledge, but also for forest management. Some forest management strategies have already been proposed to enhance Mediterranean forests' growth productivity under dry conditions and to adapt them to climate change, in particular through the reduction of competition among trees by thinning (Aldea *et al.*, 2017; Bréda *et al.*, 1995; Calev *et al.*, 2016; Sohn *et al.*, 2016; Vilà-Cabrera *et al.*, 2018).

Ecological competition is defined as a negative interaction between plants, which can be direct (direct contact, allelopathy) or indirect through the use of common resources (Connell, 1990), and can be intraspecific or interspecific. Thus, competition defines the pattern of net resource availability and is largely responsible for differences in individual growth among trees with varying social status and neighbourhoods (Calama *et al.*, 2019). Competition is considered symmetric when competitors share resources in proportion to their size, while competition is considered to be asymmetric when large competitors capture a disproportionate share of contested resources over smaller competitors (Schwinning & Weiner, 1998). On one hand, trees' modes of competition are driven by environmental factors and are linked to the most prevailing limiting factor (limitation-caused matter partitioning hypothesis; Pretzsch & Biber, 2010). Competition for belowground resources is often assumed to be symmetric – like in water-limited ecosystems (Pretzsch & Biber, 2010) e.g. Mediterranean ecosystems – while competition for light is asymmetric due to the directional component of light (Schwinning & Weiner, 1998). On the other hand, competition also modulates individual tree response to drought. For example, the reduction of competition by thinning tends to increase stand-level water availability (Bréda *et al.,* 1995) and may alleviate drought-related reductions in tree growth (e.g., Aldea *et al.*, 2017; Gavinet *et al.*, 2015; Olivar *et al.*, 2014; Sohn *et al*., 2016). In addition, trees can have various responses to drought depending on the species, their size and

social status. Some studies have demonstrated that large trees are less resilient to drought than smaller trees (Castagneri *et al*., 2012; Sánchez-Salguero *et al*., 2015; Zang *et al*., 2012) while other studies have found the opposite pattern (Calama *et al.*, 2019; Martin-Benito *et al.*, 2011; Trouvé *et al.*, 2017) or no difference between dominant and suppressed trees (Bello *et al.*, 2019; Lebourgeois *et al.*, 2014). These contrasting results can be explained by species-specific differences in shade- and drought-tolerance strategies, and by differences in the population and site characteristics, especially in the stand water balance, whose spatiotemporal dynamics is often not well quantified or considered.

Considering the various relationships between competition and drought and their impacts on tree radial growth, models that aim to accurately predict individual tree growth or stand-scale productivity should take into account both competitive and climatic drivers at an annual resolution (Ameztegui *et al.*, 2017). Including these drivers is important to correctly simulate (i) decadal and multi-decadal growth trends, which are strongly influenced by competition, (ii) the impacts of human and natural disturbances on the spatial arrangement of the stand and on the competition intensity experienced by each tree (e.g. after thinning or massive mortality), and (iii) the interannual variability in tree growth, which is mainly controlled by interannual climate variability (Calama *et al.*, 2019; Condés & García-Robredo, 2012; Rathgeber *et al.*, 2005; Sánchez-Salguero *et al.*, 2015). This is especially important to improve empirical forest growth models that statistically link growth data with specific site and climatic conditions. Though empirical models are difficult to extrapolate, they are very precise under their calibration domain and are widely used for forest management planning (e.g. growth and yield models; see Weiskittel Jr *et al.*, 2011).

Several types of indices can be used in such empirical forest growth models to assess the competition and water stress experienced by a tree. Competition indices are often used to investigate the different modes of competition (Biging & Dobbertin, 1995; Prévosto, 2005). For example, asymmetric competition for light can be predicted using competition indices that derive from tree heights and crown sizes, while symmetric competition for belowground resources can be predicted using competition indices based on tree diameters, root mass, or rooting depths (Pretzsch *et al.*, 2017). Many drought indices have been developed for modelling purposes. Speich (2019) classified these drought indices into four levels, from the least to the most integrative: (1) based on precipitation, (2) based on evaporative demand, (3) based on soil moisture storage and stand properties, and (4) based on physiological thresholds. Drought indices that are more mechanistic generally perform better at predicting tree growth than indices including precipitation and evaporative demand, or precipitation alone (Speich,

119 2019) as they better represent the actual water available for the plants (3 and 4) and the drought intensity they have

120 experienced (4).

121   In this study, we developed an empirical mixed modelling approach to predict individual Aleppo pine

122 (*P.halepensis* Mill.) radial growth based on its size, neighbourhood, and climatic factors. We used five competition

123 indices (CIs) that are derived from different types of information in order to investigate the modes of competition

124 of *P.halepensis*. Several water stress indices (WSIs), with contrasting levels of information were also used to

125 investigate the influence of water stress induced both by soil and climatic factors on *P.halepensis* radial growth.

126 We especially aimed at evaluating the potential of competition indices (CIs) and water stress indices (WSIs) jointly

127 for predicting annual basal area increment (BAI) in *Pinus halepensis* under different thinning intensities, and

128 selecting the best CI and WSI indices. Our main hypothesis were, as follows:

129   (i)   *P.halepensis'* main mode of competition is symmetric;

130   (ii)   Soil water availability is a better predictor of *P.halepensis* growth than rainfall alone;

131   (iii)   The best pine growth model includes both competition indices and water stress indices.

132

133 **2.   MATERIAL AND METHODS**

134 *2.1. Study site and experimental design*

135

136   This study was conducted in Southern France in the 'Saint Mitre' experimental site, which is located

137 about 30 km west of Marseille (43°27'0"N; 5°2'24"E). The area is flat and at a mean altitude of 130 m above sea

138 level. The climate is Mediterranean, with warm, dry summers and cool, wet winters. The mean annual temperature

139 is 15.3°C and mean annual precipitation is 562 mm (Istres weather station, 1985-2014; Appendix A). However,

140 fluctuations in rainfall are frequently observed between years. For example, 2015 and 2016 received 660 mm and

141 411 mm of rainfall, respectively. Soils are calcareous, with a sandy-loam texture (55% sand, 30% silt and 15%

142 clay) and a mean depth of 60 cm before reaching the calcareous bedrock. The site is composed of a monospecific

143 even-aged (~60 years old) Aleppo pine forest (*Pinus halepensis* Mill.) that has naturally regenerated after

144 agricultural abandonment ~60 years ago. The understorey is mainly composed of Mediterranean oaks (*Quercus*

145 *ilex* and *Quercus coccifera*), shrubs (e.g. *Phillyrea angustiflia*, *Rosmarinus officinalis*) and scarce herbaceous

146 plants (e.g. *Brachypodium retusum*).

147   Natural pine stands were thinned in 2007, leading to three different pine cover treatments and thus

148 different competition situations: (i) light pine cover (basal area: 10.2 m².ha⁻¹), (ii) moderate pine cover (19.2

5

149 m²/ha), (iii) dense pine cover (32.0 m²/ha; no thinning). Each treatment was replicated in four 25m × 25m plots

150 (Appendix B). All pines were individually identified, geo-referenced in spring 2017 using a differential GPS

151 (Trimble© TSC2, Trimble Inc, USA) and a laser distance meter (LaserAce® 300, Measurements Devices Ltd,

152 UK). Their circumference at breast height (1.30m) and their height were measured in 2017 using a measuring tape

153 and a rangefinder (Vertex III, Häglof, Sweden), respectively.

154

155   *2.2. Measurement of individual tree growth based on ring-width series*

156

157   From September to October 2017, 1-2 cores were extracted at breast height using a Pressler increment

158 borer from 15 randomly selected (co-)dominant Aleppo pines in the inner part of each of the 12 plots (20m*20m,

159 to reduce border effect, Appendix C). Cores were mounted and sanded until ring boundaries were clearly visible.

160 We used the WinDENDRO program (WinDENDRO™ 2014, © Regent Instruments Canada Inc.) to measure ring

161 widths at a resolution of 0.034 mm and visually cross-date each individual chronology. We removed the series

162 that could not be accurately cross-dated (e.g. due to high polycyclism rate and/or high number of missing rings).

163 Most of the removed trees were in the dense cover treatments, however at the end the distribution of individuals

164 within the treatments was even (dense cover: 62 individuals; moderate cover: 58 individuals; light cover: 55

165 individuals). In order to have a single series per tree, chronologies were averaged for each individual tree when

166 two of them were available. This resulted in 175 individual tree-ring width series that were retained for the

167 following analyses.

168   To correct the trend associated with the geometrical constraint of adding a volume of wood to a stem of

169 increasing radius, the tree-ring width series were converted into basal area increments (BAI) (Biondi & Qeadan,

170 2008) using the following formula:

171

172   [1] $BAI = \pi(r_t^2 - r_{t-1}^2)$

173

174 With r_t^2 and r_{t-1}^2 referring to the stem radii corresponding to years *t* and *t-1*, respectively.

175 The BAI was then used to represent the annual individual tree growth. Only the data from 2008 to 2017 were used

176 for the analyses, as the structure of the thinned stands was not known before that date.

177

178

6

179

180 *2.3. Selection of the competition indices*

181

182   Competition was quantified using competition indices (CIs). CIs can also be classified into two

183 categories: distance-dependent CIs based on the relative dimensions and the distance of a subject tree to its

184 neighbours within a given radius; and distance-independent CIs based only on non-spatial and aggregated

185 information on tree size and the number of trees in a given area. We used 5 different CIs based on the literature,

186 using different types of information (distance, circumference, height) in order to compare their predictive power

187 and to investigate the dominant mode of competition (symmetric or asymmetric). In this study, we tested three

188 distance-dependent indices (*HEG* to *VER*), and two distance independent indices (*RS* and *BAL*). The first CI (*HEG*)

189 is a distance weighted size-ratio index, developed by Hegyi (1974). Because it uses tree circumferences, it is

190 expected to account for symmetric competition:

191

192   [2]
$$HEG = \sum_{\substack{j=1 \\ j \neq i}}^{n} \frac{C_j^2}{C_i^2 . dist_{ij}}$$

193

194 C_i is the circumference at breast height of the subject tree *i*, C_j is the circumference of the neighbour tree *j*, and

195 *dist* is the distance between both trees *i* and *j*.

196 The second and third indices were developed by Pukkala & Kolström (1987). They are based on the sum of

197 horizontal or vertical angles that originate from the subject tree, spanning the circumference or the top of the crown

198 of each neighbour tree (*HOR* and *VER*), respectively. *HOR is* based on the circumferences of all neighbours, and

199 is expected to account for symmetric competition. In contrast, *VER* uses the height of taller neighbours and is

200 expected to account for asymmetric competition:

201

202   [3]
$$HOR = \sum_{\substack{j=1 \\ j \neq i}}^{n} 2. \arctan(\frac{C_j}{2.\pi.dist_{ij}})$$

203

204   [4]
$$VER = \sum_{\substack{j=1 \\ j \neq i \\ H_j > H_i}}^{n} \arctan(\frac{H_j - H_i}{dist_{ij}})$$

205   With H_i and H_j corresponding to the heights of the subject and of the neighbour tree, respectively.

206   The fourth index is the Relative Spacing (*RS*) index developed by Schröder & Gadow (1999). This index is

207   computed at the plot scale, which leads to a single plot-level value:

208

209   [5] $$RS = \frac{\sqrt{10000/N}}{H_d})$$

210

211   With N the number of stems per hectare and H_d the dominant stand height. The dominant stand height is usually

212   defined as the height of the 100 tallest trees in one hectare; however for our study we took the 5 tallest trees in

213   each plot.

214   The last index was first developed by Wykoff *et al.* (1982), and corresponds to the total basal area of trees that are

215   larger than the subject tree (also called Basal Area of Larger trees; *BAL*). It is expected to account for asymmetric

216   competition as only large trees are taken into account, but also for symmetric competition, as it is size-related:

217

218   [6] $$BAL = \sum_{\substack{j=1 \\ j \neq i \\ C_j > C_i}}^{n} \frac{C_j^2}{4\pi}$$

219

220   We computed the values of the distance-dependent competition indices (HEG, HOR, VER) for different

221   competition radii (from 1 meter to 8 meters), and then calculated the correlation coefficients between the mean

222   BAI for 10 years and the competition index. We then selected a competition radius of 5 meters for the three

223   distance-dependent indices (see Appendix D). In total, we produced five competition indices for each individual

224   tree. We did not have height and circumference data for all individual trees between 2008 and 2017, but as the

225   stands are quite homogeneous and major changes in the stand composition and structure did not occur between

226   2007 and 2017 (Appendix F) we made the very likely assumption that individual CIs remained constant over this

227   period.

228

229   *2.4. Water Balance model*

230

231   The effects of the climate, stand, and soil properties on drought characteristics can be integrated into a

232   forest water balance model. We thus developed a two-strata forest water balance model, i.e. over- and understorey
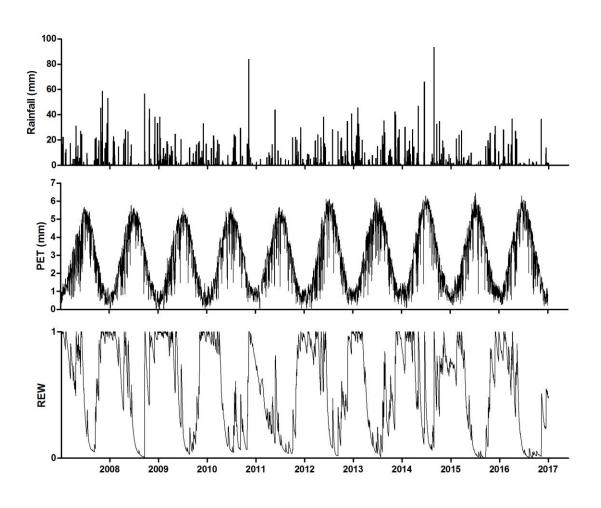
8

233 are considered (adult tree canopy only composed of Aleppo pines; shrubby mixed understorey), based on Granier

234 *et al*., (1999), which computes daily variations in soil water content. The model uses daily temperatures and rainfall

235 data as inputs, and some site and stand parameters such as soil depth, maximum and minimum extractable soil

236 water (from soil texture analyses), fine root distribution, soil porosity, and stand Leaf Area Index (LAI). Istres

237 weather station (12 km NW of the site) provided the climatic data over the entire study period and global radiation

238 data came from Marignane station (14km E of the site). The PET was computed using the radiation-based method

239 of Turc (Turc, 1961) in the absence of wind data recorded on-site. Soil samples were collected in 2014 and 2017.

240 In 2014, 2 plots per treatment were sampled; in each of the selected plots 6 soil samples at three soil depths were

241 collected for texture analysis. In 2017, 5 soil pits were dug into the treatments and 30 soil samples of constant

242 volume (3 soil depths and 2 samples per depth) were collected to measure the bulk density, the content in coarse

243 elements and in fine roots (Table 1). The soil properties were considered as constant among the plots, except for

244 soil depth. Water buckets were computed for each soil layer (Jabiol *et al.*, 2009) and aggregated at the plot scale.

245 Transmitted radiation was measured every minute for 48 hours during two successive clear days of April 2017 in

246 9 plots (3 plots/treatment) using 6 solarimeter tubes (PAR/LE Solems) per plot and 2 solarimeter tubes in open

247 conditions, in order to compute transmitted radiation. Based on this transmitted radiation, LAI was then calculated

248 using the Norman & Jarvis (1975) equations. A relationship between stand basal area and the LAI values was

249 established to model the changes of LAI through time. The LAI was later used to compute the rainfall interception

250 of the Aleppo pine canopy and the understorey using the model proposed by Molina & del Campo (2012). Rainfall

251 interception, transpiration of the two strata, and the soil water dynamics were computed and provided daily

252 variations of soil water content and relative extractable water (Prévosto *et al.*, 2018) (REW, daily extractable water

253 standardized by maximum water extractable; Figure 1).

254

255 *Table 1: Soil characteristics incorporated for each layer of each plot in the water balance model. Only variations*

256 *in layer thickness was incorporated within plots.*

Soil characteristics	Layer 1	Layer 2	Layer 3
Fine roots (%)	58.4	22.4	19.2
Coarse elements (%)	9.5	8.9	8.9
Bulk density (g/cm^3)	1.33	1.44	1.56
Sand (%)	53.8	52.8	49.7
Clay (%)	12.5	15.03	16.04

Silt (%)				34.5				32.1				34.4	
Plot number	**1**	**2**	**3**	**4**	**5**	**6**	**7**	**8**	**9**	**10**	**11**	**12**
Soil total depth (cm)	58	38	64	69	68	61	66	59	57	71	67	43
Layers thickness (cm)	19.3	12.7	21.3	23	22.7	20.3	22	19.7	19	23.7	22.3	14.3

257

258

259 *Figure 1: Variations in rainfall, potential evapotranspiration (PET) and relative extractable water (REW) calculated using the*

260 *water balance model from between 2008 and 2017.*
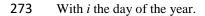
261 *2.5. Water stress indices (WSI)*

262

263 For each plot and each year, we used four different WSIs using different levels of information i.e. soil

264 and/or climatic constraints. The first three WSIs derive from the forest water balance to account for climate and

265 local conditions, while the fourth WSI derives directly from climatic data. We assumed that a drought had occurred

266 when the soil REW dropped below a threshold of 0.4, as proposed by Granier *et al.* (1999), a threshold that has

267 been successfully applied in other empirical and modelling studies (Bello *et al.*, 2019; Forner *et al.*, 2018; Granier

268   *et al.*, 2007; Speich, 2019). The first WSI cumulates the daily differences between REW and the 0.4 threshold of

269   REW, and indicates both drought intensity and duration (*INT*, Figure 3):

270

271   [7] $INT = \sum(0.4 - REW_i)$ for $REW_i \leq 0.4$

272

273   With *i* the day of the year.

274   The second WSI only represents the drought duration (*DUR*) and corresponds to the number of days that REW is

275   below 0.4 (Figure 2). The third WSI accounts for drought duration and timing (*TIM*), and was adapted from the

276   seasonal water stress index developed in Mina *et al.* (2016). For each season, we produced an intermediate WSI,

277   which is the number of water stress days divided by mean soil water content ($\overline{SWC}$) during the given period. We

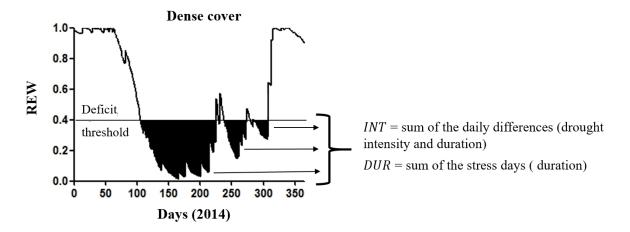278   then totalled all of the seasonal WSIs to obtain the annual WSI:

279

280   [8] $TIM = \sum(\frac{Number\ of\ WS\ days}{\overline{SWC}})_{season}$

281

282   The fourth WSI corresponds to annual rainfall (*RAIN*). Many studies have used seasonal rainfall instead of annual

283   rainfall when investigating *P. halepensis* radial growth (i.e. Olivar *et al.*, 2012; Pasho *et al.*, 2012), however after

284   preliminary analyses, we found that for our study site, annual rainfall was a better predictor of growth than seasonal

285   rainfall (Appendix A).

286

287

288

289   *Figure 2: Graphical explanation of the WSIs construction. Example for year 2014. REW does not start at 1 every year, it goes*

290   *on from year to year.*

291   We did not include temperatures in our model for two reasons. Firstly, *P.halepensis* is thermophilous and

292   is thus expected to be sensitive to cold temperatures, which could negatively affect its growth. However, such

293   temperatures are not seen at our study site (Appendix A). Secondly, during preliminary analyses, annual minimum

294   and maximum temperatures were found to be poor predictors of tree growth and were thus removed from the final

295   analyses (Appendix D).

296

297   *2.6. Statistical analyses, growth models and indices selection*

298

299   Kruskal-Wallis non-parametric tests followed by Dunn's test were performed to explore the effect of the

300   cover treatments on BAI, using the *{dunn.test}* package (Dinno, 2017) from the open-source R statistical software

301   (R Core Team, 2017).

302   Simple linear regressions were used to explore the relationships between tree BAI and the different

303   CIs/WSIs. To jointly test the influence of both competition and water stress on *P. halepensis* tree growth, we

304   developed linear mixed-effect models using the *{lme4}* and *{lmerTest}* packages (Kuznetsova *et al.*, 2017). Natural

305   logarithm transformations were used to satisfy the assumptions of linearity and normality of the residuals, the

306   'LogSt' function from the *{DescTools}* package (Signorell *et al.*, 2019) being specifically used to account for null

307   CI values. This led to the following model equation:

308

309   [9] $$\log\left(BAI_{i,t}\right) = k + \propto \log\left(BA_{i,t-1}\right) + \beta \log(CI_i) + \gamma \log(WSI_t) + \delta_i + \varepsilon$$

310

311   Where k, $\propto$, β and γ are the fixed parameters, $BAI_{i,t}$ the basal area increment (mm²) of the tree i during the year t,

312   $BA_{i,t-1}$ the tree basal area of previous year $t-1$ (m²), CI_i a competition index, WSI_t a water stress index of the year

313   t, δ_i the random effect estimated for the intercept with tree as a grouping factor, and ε is the residual error. BA was

314   included in the models to account for the effect of tree size on current annual growth. We included trees nested

315   into the plot, plots alone, or trees alone as a random effect on the intercept term; however after preliminary analysis

316   we retained the tree random effect alone as it performed better. Similarly, we added a tree random effect on the

317   parameters (slope), however all of these random effect models failed to converge. Finally, the tree random effect

318   on the intercept term was the only to be retained. We also investigated the interaction between competition and

319   water stress, but the interaction was not significant and only the additive models were retained.

320   All of the possible combinations of CIs and WSIs as explanatory variables were tested, and the optimal CI

321   and WSI were selected using the Akaike's Information Criterion (AIC) with maximum likelihood fitting (MLE)

322   as only our fixed effects differed between models. The parameters of the best model were fitted using restricted

323   maximum likelihood (REML). We used the marginal r-squared (variance explained by the fixed effects only) and

324   the conditional r-squared (variance explained by both fixed and random effects) using the R package *{MuMIn}*

325   (Barton, 2018) as indicators of model performance. The marginal r-squared of the best model were bootstrapped

326   using the R package *{boot}* to produce confidence intervals and to evaluate the model's robustness (Canty &

327   Ripley, 2019; Davison & Hinkley, 1997). The bootstrap was stratified (strata: individual tree) and based on 2000

328   replicates. Conditional r-squared were not used for the bootstrap, as this method does not correctly estimate the

329   variance in a random effect model, in particular when the variables are not independent and identically distributed

330   (McCullagh, 2000).The normality of the residuals and multicollinearity of the explanatory variables were tested

331   using Shapiro-Wilk test and the Variance Inflation Factor, respectively. To evaluate the effect of the selected

332   variables on the standardized-BAI, effect plots were produced using the R package *{effect}* (Fox & Weisberg,

333   2018a, 2018b).

334

335   **3.   RESULTS**

336   *3.1. Temporal variability in tree BAI*

337

338   Over the 2008-2017 study period, there was a consistent increasing gradient of BAI from the control to

339   the light cover treatment (Figure 3), confirmed by the Kruskal-Wallis test and Dunn's test: significant differences

340   were found between the three treatments for all years (Kruskal-Wallis statistics: Chi square = 466.99, df = 2, p-

341   value < $2.2e^{-16}$). There was high variability between years with 2016 and 2017 being the least productive years.
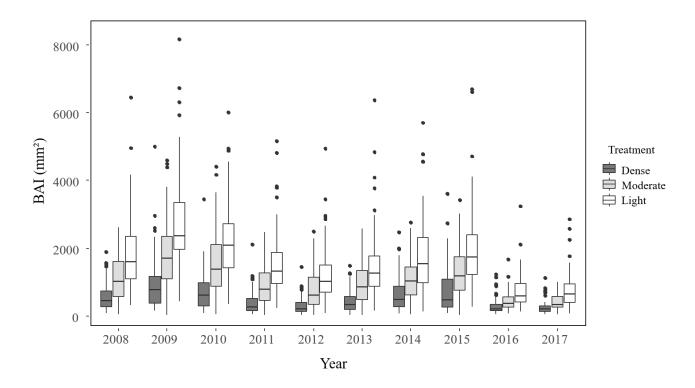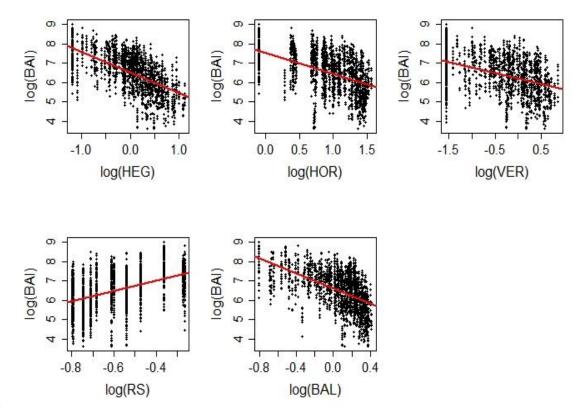
Figure 3: Variations of tree basal area increment (BAI ; mm²) between 2008 and 2017 among the cover treatments resulting from different thinning intensities (Dense, Moderate, Light). Medians, 1st and 3rd quartiles are presented. Decline in growth in 2016 and 2017 is a climatic trend, these years being both extremely dry (411mm and 311mm, respectively).

3.2. Linear regressions with one-single explanatory variable

BAI was negatively correlated with the CIs 1, 2, 3 and 5 – indicating that the higher the competition experienced by the tree is, the lower its growth rates are (Figure 4, r^2 from 0.218 to 0.377). On the contrary, when *RS* increased (the relative spacing between trees), the BAI increased as well: the wider the spacing between trees is, the greater the BAI is ($r^2 = 0.209$).

354

Figure 4: Tree Basal Area Increment (BAI) relative to Competition Indices (CIs). Curve fits in the graphs are separate linear

regressions, from HEG to BAL: log(BAI) = -1.063 log(HEG) + 6.517, r² = 0.377; log(BAI) = -1.078 log(HOR) + 7.520, r² = 0.228;

log(BAI) = -0.582 log(VER) + 6.200, r² = 0.218; log(BAI) = 2.657 log(RS) + 8.068, r² = 0.209; log(BAI) = -1.925 log(BAL) + 6.612,

r² = 0.291. All slopes are significantly different from zero (p < 0.001)

As indicated by the different linear regressions, there was a negative relationship between the BAI and

the WSIs (except for *RAIN*; Figure 5), which indicates that when the water stress increases, the BAI decreases (r²

from 0.248 to 0.260). In contrast, when rainfall increases (*RAIN*) the BAI increases as well, though the relationship
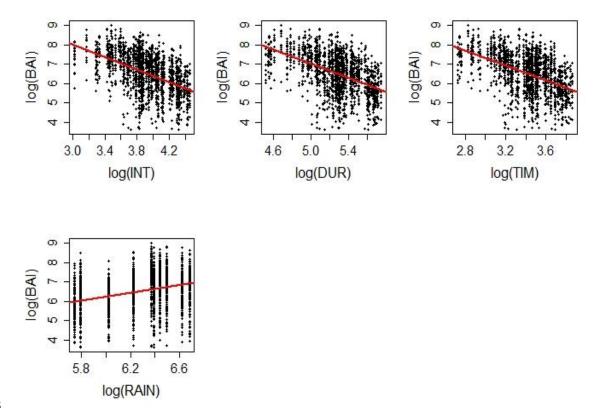
is weaker (r² = 0.101).

363

Figure 5: Tree Basal Area Increment (BAI) relative to Water Stress Indices (WSIs). Curve fits in the graphs are separate linear

regressions, from INT to RAIN: log(BAI) = -1.657 log(INT) + 13.020, r² = 0.255; log(BAI) = -1.813 log(DUR) + 16.074, r² = 0.260;

log(BAI) = -1.915 log(TIM) + 13.077, r² = 0.248; log(BAI) = 1.032 log(RAIN) + 0.049, r² = 0.101. All slopes are significantly

different from zero (p < 0.001)

3.3. Linear mixed-effects models with multiple explanatory variables: selection of the indices

For the single variable models, *HEG* (Hegyi competition index) and *DUR* (number of days that trees experienced water stress) were the best explanatory indices (38% and 16% of the variance explained, respectively). *HEG* and *DUR* were still the best predictors when BA was included in the mixed models (38% and 53% of the variance explained by the *HEG* and *DUR* models, respectively). However, WSIs and BA combined were better predictors of growth than CIs and BA together (*RAIN* excluded), the marginal R² ranged from 43% to 53% for the WSIs and from 30% to 40% for the CIs, respectively. When three explanatory variables were included, the best five models included BA, *DUR* and different variants of the CIs (Table 2). In the best model, *BAL* – sum of the basal area of larger trees – and *DUR* – the number of water stress days – were selected together. The fixed effects

379   of this model explained 56% of the total variance (marginal r-squared), with a narrow confidence interval (0.516-

380   0.576; obtained from bootstrapping), highlighting its low dependency on the characteristics of the input dataset

381   and its high robustness. Finally, the inclusion of the random effect considerably improved the models explaining

382   a large proportion of the remaining variance (e.g. 22% for the best model).

383

384   *Table 2: Linear mixed-effects models of the annual tree basal area increment (BAI) as a function of the basal area of the*

385   *previous year (BA) and the different indices produced previously (CI and WSI). Selected models are in bold in their group; the*

386   *final selected model is in bold and red.*

Models (with tree as a random effect on the intercept)	Marg. R²	Cond. R²	AIC	Δ*i*
log(BAI) ~ log(*HEG*)	**0.378**	**0.678**	**3438.12**	**0.00**
log(BAI) ~ log(*BAL*)	0.291	0.677	3478.62	40.50
log(BAI) ~ log(*VER*)	0.229	0.677	3502.86	64.74
log(BAI) ~ log(*HOR*)	0.219	0.677	3506.58	68.46
log(BAI) ~ log(*RS*)	0.210	0.677	3509.45	71.33
log(BAI) ~ log(*DUR*)	**0.161**	**0.776**	**2798.09**	**0.00**
log(BAI) ~ log(*INT*)	0.154	0.770	2839.22	41.12
log(BAI) ~ log(*TIM*)	0.149	0.768	2853.73	55.64
log(BAI) ~ log(*RAIN*)	0.102	0.790	2893.81	95.72
log(BAI) ~ log(BA) + log(*HEG*)	**0.376**	**0.899**	**3276.37**	**0.00**
log(BAI) ~ log(BA) + log(*BAL*)	0.328	0.908	3303.17	26.79
log(BAI) ~ log(BA) + log(*HOR*)	0.305	0.929	3366.63	90.26
log(BAI) ~ log(BA) + log(*VER*)	0.309	0.931	3373.32	96.95
log(BAI) ~ log(BA) + log(*RS*)	0.304	0.935	3390.50	114.13
log(BAI) ~ log(BA) + log(*DUR*)	**0.527**	**0.755**	**2704.38**	**0.00**
log(BAI) ~ log(BA) + log(*TIM*)	0.516	0.745	2761.41	57.04
log(BAI) ~ log(BA) + log(*INT*)	0.434	0.719	2802.18	97.80
log(BAI) ~ log(BA) + log(*RAIN*)	0.125	0.877	2885.25	180.88
log(BAI) ~ log(BA) + log(*BAL*) + log(*DUR*)	**0.556**	**0.773**	**2672.26**	**0.00**
log(BAI) ~ log(BA) + log(*HEG*) + log(*DUR*)	0.561	0.781	2681.25	8.99
log(BAI) ~ log(BA) + log(*VER*) + log(*DUR*)	0.561	0.781	2681.25	8.99
log(BAI) ~ log(BA) + log(*HOR*) + log(*DUR*)	0.547	0.767	2691.22	18.96

log(BAI) ~ log(BA) + log(RS) + log(DUR)	0.542	0.765	2701.21	28.95
log(BAI) ~ log(BA) + log(BAL) + log(TIM)	0.545	0.764	2729.16	56.90
log(BAI) ~ log(BA) + log(HEG) + log(RAIN)	0.424	0.854	2731.59	59.33
log(BAI) ~ log(BA) + log(VER) + log(RAIN)	0.424	0.854	2731.59	59.33
log(BAI) ~ log(BA) + log(HEG) + log(TIM)	0.552	0.773	2735.99	63.73
log(BAI) ~ log(BA) + log(VER) + log(TIM)	0.552	0.773	2735.99	63.73
log(BAI) ~ log(BA) + log(BAL) + log(INT)	0.481	0.770	2742.56	70.30
log(BAI) ~ log(BA) + log(HEG) + log(INT)	0.505	0.788	2742.82	70.56
log(BAI) ~ log(BA) + log(VER) + log(INT)	0.505	0.788	2742.82	70.56
log(BAI) ~ log(BA) + log(HOR) + log(TIM)	0.537	0.758	2747.50	75.23
log(BAI) ~ log(BA) + log(RS) + log(TIM)	0.533	0.756	2756.83	84.57
log(BAI) ~ log(BA) + log(BAL) + log(RAIN)	0.344	0.865	2767.70	95.43
log(BAI) ~ log(BA) + log(HOR) + log(INT)	0.471	0.751	2773.10	100.84
log(BAI) ~ log(BA) + log(RS) + log(INT)	0.469	0.746	2788.17	115.91
log(BAI) ~ log(BA) + log(HOR) + log(RAIN)	0.281	0.865	2816.03	143.77
log(BAI) ~ log(BA) + log(RS) + log(RAIN)	0.273	0.852	2829.26	157.00

387 *Abbreviations: Marg. R² the marginal r-squared (accounting for the fixed effects); Cond. R² the conditional r-squared*

388 *(accounting for the fixed and random effects); AIC the Akaike Information Criterion; Δi the difference in AIC with respect to*

389 *the best fitting model of each category delimited by plain black lines.*

390

391 *Table 3: Estimated coefficients, standard errors (Std. errors) and p-values for the best model. The variances of ε_{ran} and ε_{res}*

392 *are shown as well.*

$\log(BAI_{i,t}) = k + \propto \log(BA_{i,t-1}) + \beta \log(BAL) + \gamma \log(DUR)$				δ_i	ε
Parameters	Estimates	Std. errors	P value	Variance	Variance
k	15.974	0.409	< 2e-16 *		
α	0.410	0.064	6.29e-10 *		
β	-1.027	0.175	1.94e-08 *	0.206	0.212
γ	-1.497	0.048	< 2e-16 *		

393 *significant correlation (p < 0.01)

394

3.4. Predicted effects of the main variables from the best model on growth

396

397 All of the variables of the best final model significantly affect individual BAI (Table 3). Basal area in the

398 previous year (BA$_{t-1}$) had a positive effect on BAI (Table 3 & Figure 6). From 0.01 m² to approximately 0.04 m²,

399 BA$_{t-1}$ had a strong positive effect on BAI. This positive effect became relatively lower with higher variability

400 between 0.04 m² and 0.10 m² due to sparse data. Both *BAL* and *DUR* had a negative effect on BAI overall. *DUR*

401 had a negative effect on BAI with low variability. *BAL* had a strong negative effect on BAI with high variability

402 between 0 and 1 and a more neutral negative effect on BAI with higher variability when *BAL* ranged between 1

403 and 3.

404

Figure 6: Predicted effects of BA$_{t-1}$, BAL, and DUR on standardised BAI estimated using the best three-variable model (table 2).

Shaded areas around the curves represent the confidences intervals of the mean (95%). Straight lines above the x-axis

represent the distribution of the measured data.

408 The relationship between BAL and DUR is only additive, which means that pine growth response to

409 drought is the same under different levels of BAL. However, BAL reduces growth, i.e. the higher the BAL the

410 lower the growth (Figure 8). For example, when drought duration equals 200 days in a year, pine trees experiencing

411 no competition at all increase annual pine growth by 1mm², while pines experiencing strong competition (BAL =

3) would decrease annual pine growth by 0.4 mm² (Figure 7). It also shows that strong competition reduces the number of water stress days pine trees can tolerate in a year before BAI is considerably affected (i.e. when standardized BAI drops below 0). In our example, when BAL = 3, standardized BAI drops below 0 after 150 water stress days. When BAL = 1, standardized BAI drops below 0 only after 200 water stress days. Finally, when BAL = 0, standardized BAI never goes below 0 (Figure 8).
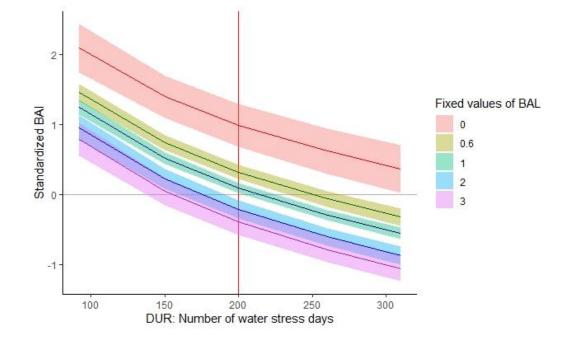

Figure 7: Predicted effects of the number of days with water stress (DUR) on standardised BAI according to different fixed values of Basal Area of Larger trees (BAL; in colors), estimated using the best three-variables model (table 2). Shaded areas around the curves represent the 95% confidences intervals of the mean effects (means are the coloured curves). The mean standardized growth (horizontal line) and the value of DUR=200 is indicated in red (vertical line) (see also comments in the text)

4. DISCUSSION

4.1. Competition indices

In this study, the Hegyi competition index (*HEG*) was selected as the best predictor of individual annual BAI among the competition indices for the one-variable and the two-variable models, followed by the basal area of larger trees (BAL; *BAL*), the angles CIs (i.e. *HOR* and *VER*), and the relative spacing CI (*RS*). This suggests that competition would mainly be symmetric, i.e. the system is limited by water. However, the *BAL* was selected as the best predictor of BAI among the CIs in the three-variable models, followed closely by the Hegyi CI (*HEG*),

and the vertical angles (*VER*). This suggests that part of the competition explained by certain CIs (i.e. *HEG*) could be taken into account by WSIs. In other words, this indicates that some CIs do indeed reflect the competition for water. The poor performance of *RS* can be explained by its generality as it provides a single competition value for all trees within a given plot, which does not accurately represent the actual competition experienced by each individual tree.

The three best CIs (*BAL*, *HEG* and *VER*) correspond to three different methods of computing competition; despite this, *BAL*, *HEG* and *VER* have similar BAI predictive power, with a marginal r-squared of about 56%. *HEG* only relies on circumference and should indicate symmetric competition for belowground resources, while *BAL* also relies on circumferences but only incorporates trees larger than the subject tree, reflecting both asymmetric and symmetric competition. *VER* uses tree height, which is more subject to measurement errors, but is more representative of competition for light (e.g. asymmetric competition) than circumference. We investigated the relationship between height and circumference. However, no clear relationship was detected (Appendix G), indicating that both represent different aspects of competition with water stress indices explaining yet another aspect of competition. It also highlights the fact that CIs can share some information, as competition can never be defined as completely size-symmetric or completely size-asymmetric (Schwinning & Weiner, 1998). Hence, our hypothesis (i) is not entirely verified: *P.halepensis'* mode of competition seems to be asymmetric, but this is contradicted by the good performance of the *HEG* index.

Moreover, *BAL* is distance-independent, while *HEG* and *VER* are distance-dependent. The fact that a distance-independent CI and distance-dependent CIs have similar predictive power is not straightforward. In most cases and especially in heterogeneous stands, distance-dependent competition indices appear to be more correlated with tree growth, as they consider the spatial arrangement of the trees within a stand (Contreras *et al.*, 2011; Pukkala & Kolström, 1987; Rouvinen & Kuuluvainen, 1997). However, results from other studies suggest that neither distance-independent indices nor distance-dependent indices perform universally better (our study; Biging & Dobbertin, 1995; Prévosto, 2005). These contrasting results suggest that a single best CI for all sites and all species may not exist. In fact, CIs are most likely species-specific, and depend on local site conditions. For example, Contreras *et al.* (2011) found that the best predictor of BAI of *Pinus ponderosa, Pseudotsuga menzisii* and *Larix occidentalis* was the horizontal angles CI. Cattaneo *et al.* (2018) found that the Hegyi CI was the best predictor of *Pinus pinea* and *Pinus halepensis* radial growth, compared to asymmetric competition indices. In our study, the stands are quite homogeneous and major changes in the stand composition and structure did not occur between 2007 and 2017 (Appendix F). Therefore, if we aim to successfully predict tree growth over a long-term,

461 and especially growth release after neighbourhood mortality, the Hegyi competition index may be more suitable.

462 However, to simulate short-term radial growth, testing several different CIs would be a valuable approach as their

463 predictive power could differ between species and stand spatial arrangements.

464

465 *4.2. Water stress indices*

466

467   Our results suggest that the growth of *P. halepensis* is largely controlled by soil water content rather than

468 annual precipitation alone, which verifies our second hypothesis and is in accordance with Alfaro-Sánchez *et al.*

469 (2018), Misson *et al.* (2004), Rathgeber *et al.*, (2005) and Vennetier *et al.* (2018). Soil water availability is more

470 biologically meaningful than annual precipitation alone, as it not only integrates water inputs (rainfall and

471 interception by the canopy), but also the soil water content (e.g., according to soil depth and texture), and water

472 loss through vegetation (evapotranspiration, which depends on PET, a combination of atmospheric temperature,

473 air relative humidity and solar radiation). Indeed, atmospheric conditions also play an important role in regulating

474 stomatal conductance. For example, Maseyk *et al.* (2008) found in the case of *P.halepensis* that, irrespective of

475 soil moisture, leaf vapour pressure deficit greatly influenced stomatal conductance when REW was above 0.2. In

476 general, vapour-pressure deficit was found to limit tree growth and was therefore advised to be considered in forest

477 models (Novick *et al.*, 2016; Sanginés de Cárcer *et al*., 2018).

478   Among the water stress indices tested, drought duration alone (*DUR*) better predicted *P. halepensis* BAI

479 than an index that combines drought timing (*TIM*), or duration and intensity (*INT*). Similarly, preliminary analyses

480 revealed that the annual water stress indices performed better than the seasonal indices tested (Appendix A), which

481 is the reason why we chose to use annual indices over seasonal indices. This would suggest that *P. halepensis* uses

482 water whenever it is available, with no distinction for the time of the year. These results were not expected as

483 drought timing is known to have a differential impact on cambial activity, and thus ring-width (Campelo *et al*.,

484 2007; Mina *et al.*, 2016, Raventós *et al.*, 2001). In the case of *P. halepensis*, Pasho *et al.*, (2012) demonstrated that

485 cumulative precipitations from winter to spring drive secondary growth of the same year. However, Rathgeber *et*

486 *al.*, (2005) found that the duration and intensity of the drought was the main predictive factor of *P. halepensis*

487 growth, although they did not investigate the effect of drought duration alone.

488   In our study, the fact that drought duration alone better predicted Aleppo pine growth than an index that

489 also integrates drought intensity could suggest that its cambial activity may be more sink-limited than source-

490 limited. In other words, it may be more limited by the drought-induced loss of cell turgor in the cambium than by

491   the carbon availability through photosynthesis and carbon reserves (Fatichi *et al.*, 2013; Lempereur *et al.*, 2015).

492   In this sink-limited approach, there is no notion of drought intensity: as soon as the REW drops below 0.4,

493   xylogenesis stops, even though the stomata can still be open and allow carbon assimilation and transpiration.

494   Indeed, there is evidence that cambial and leaf growth are inhibited sooner than photosynthesis when water stress

495   increases (Hsiao *et al.*, 1976; Lempereur *et al.*, 2015; Muller *et al.*, 2011; Tardieu *et al.*, 2011).

496   As *P. halepensis* is known to strongly control its transpiration through stomata closure, a strategy to

497   reduce water stress (Melzack *et al.*, 1985), we could also hypothesise – as another way of explaining our results –

498   that *P. halepensis* closes its stomata as soon as there is water stress, and thus stops growing. However, Maseyk *et*

499   *al.* (2008) found that *P. halepensis* transpiration follows the same trend as described in Granier *et al.* (1999):

500   transpiration decreases linearly after reaching REW = 0.4. This threshold therefore seems accurate when looking

501   at tree transpiration; however, it might not be appropriate when linking it to tree growth. Despite the fact that *P.*

502   *halepensis* is well studied (Baquedano & Castillo, 2007; Froux *et al.*, 2005; Hover *et al.*, 2017; Klein *et al.*, 2011;

503   Melzack *et al*., 1985; Ungar *et al.,* 2013), there is a need for more physiological studies investigating the non-

504   linear, threshold-based relationship between secondary growth and drought for this species. To achieve this,

505   several different approaches could be envisaged, such as using photosynthetic rate as a proxy for carbon

506   assimilation, or by investigating water-use efficiency. A promising approach would be to investigate the link

507   between cambial activity and drought stress experienced by the tree by combining leaf water potential (Ψ_{pd}) and

508   dendrometer data that has been pre-analysed to remove shrinking-expansion phases arising from changes in the

509   water content in the elastic tissue of the stem (Balducci *et al.*, 2019; Zweifel *et al.*, 2006). For instance, Lempereur

510   *et al.* (2015) found that the summer interruption of *Quercus ilex* growth was associated with a threshold of -1.1

511   MPa and remained nil for values of Ψ_{pd} ranging from -1.1 to -4 MPa, well before transpiration ceased and

512   cavitation occurred.

513   Finally, our results suggest that water availability is a better predictor of annual tree growth than

514   competition alone, which can be explained by high climatic interannual variability, while CIs remained constant.

515   Our findings also suggest that WSIs and CIs together are the best predictors of Aleppo pine radial growth,

516   confirming our final hypothesis (iii).

517

518

519

520

4.3. Inter-individual variability

522

523   Finally, as indicated by the large proportion of the variance explained by the random effect of the tree

524   individual on the intercept (22% for the best model), there was a high inter-individual variability in *P. halepensis*

525   radial growth within our study population. The Western European population of *P. halepensis* is considered to

526   have very low genetic diversity (Soto *et al.*, 2010). However, it has high phenotypic plasticity, which has been

527   demonstrated many times for various traits at different spatial scales and climatic conditions (Baquedano *et al.*,

528   2008; Choat *et al.*, 2018; de Luis *et al.*, 2013; Rathgeber *et al.*, 2005; Vizcaíno-Palomar *et al.*, 2016; Voltas *et al.*,

529   2015; Voltas *et al.*, 2018). In our study, all *P. halepensis* individuals were within the same forest area and were

530   approximately the same age; we can therefore assume that they are part of the same genetic population. The high

531   variability in individual tree growth could therefore be explained by phenotypic variations that arose due to the

532   micro-local heterogeneity in abiotic and biotic factors, which could not be investigated in this study (e.g., presence

533   of pathogens, varying water availability at the individual level due to small-scale changes in slope or soil properties

534   and that is not considered in the WSIs). For example, we considered the understorey as a uniform patch *ergo* the

535   competition applied by the understorey was also considered to be uniform. These results highlight the importance

536   of considering variations in local conditions to accurately represent existing environmental heterogeneity (Ettl &

537   Peterson, 1995).

538

539   *4.4. Management perspectives*

540

541   The importance of thinning has already been supported by many other studies investigating forest

542   management practices for adaptation to climate change (Aldea *et al.*, 2017; Calev *et al.*, 2016; Millar *et al.*, 2007;

543   Olivar *et al.*, 2014; Vilà-Cabrera *et al.*, 2018). In particular, thinning has been found to have a positive effect on

544   biomass accumulation of young Aleppo pines, which is even more marked at dry sites (Alfaro-Sánchez *et al.*,

545   2015). However, the results available in the literature are not as clear when looking at the effects of thinning on

546   microclimatic variables. For instance, forest thinning has been found to have a limited impact on

547   evapotranspiration (Liu *et al.*, 2018), which was explained by the rapid recovery of understorey vegetation in the

548   thinned plots. The importance of accounting for understorey evapotranspiration was also highlighted by Simonin

549   *et al.* (2007) who found a substantial contribution of understorey evapotranspiration to stand evapotranspiration.

550   Mediterranean forests often present a well-developed shrubby understorey which influences the microclimate

551 (Prévosto *et al.*, 2019) and therefore needs to be taken into account for forest management. Our empirical growth

552 model integrates this understorey layer and all of the variables associated with it (evapotranspiration, transpiration,

553 rainfall interception) to compute the soil water availability at the stand level. Because water-stress was quantified

554 through a soil water budget model based on functional processes, this model can provide useful insights to forest

555 managers despite the fact that it was calibrated on a short time period and at a single site. Firstly, managers should

556 focus on soil water storage rather than precipitations alone to quantify drought situations. This is clearly more

557 complicated, but the use of forest models can be a useful alternative for assessing soil moisture and predicting tree

558 growth. Our empirical pine tree growth model can provide useful information for forest managers of

559 Mediterranean forests. For example, with ongoing climate change, the number of water stress days is expected to

560 increase (IPCC, 2014) and according to our model, this will correspond to an abrupt decline in tree annual growth

561 if the number of water stress days exceeds roughly 200 days (Figure 6). Our results suggest that reducing

562 competition by thinning could alleviate the negative effect of drought (Figure 7). For example, in dense stands

563 with a mean BAL = 3 (corresponding to our dense cover), 150 days of drought in a year is already predicted to

564 lead to an abrupt decline in tree growth in our conditions. Thinning dense stands, leading to moderate to light cover

565 (mean BAL = 1) would reduce the impact of the water stress and increase annual pine growth by 0.7 mm². This

566 study further highlights the positive effects of thinning, especially in regard to alleviating drought-related stress.

567

574

575 **5. BIBLIOGRAPHY**

576

577 Aldea, J., Bravo, F., Bravo-Oviedo, A., Ruiz-Peinado, R., Rodríguez, F., & del Río, M. (2017). Thinning enhances the species-

578 specific radial increment response to drought in Mediterranean pine-oak stands. *Agricultural and Forest Meteorology*,

579 *237–238*, 371–383. https://doi.org/10.1016/j.agrformet.2017.02.009

580 Alfaro-Sánchez, R., Camarero, J. J., Sánchez-Salguero, R., Trouet, V., & Heras, J. de Las. (2018). How do Droughts and

581 Wildfires Alter Seasonal Radial Growth in Mediterranean Aleppo Pine Forests? *Tree-Ring Research*, *74*(1), 1–14.

582   https://doi.org/10.3959/1536-1098-74.1.1

583 Alfaro-Sánchez, R., López-Serrano, F. R., Rubio, E., Sánchez-Salguero, R., Moya, D., Hernández-Tecles, E., & De Las Heras,

584   J. (2015). Response of biomass allocation patterns to thinning in Pinus halepensis differs under dry and semiarid

585   Mediterranean climates. *Annals of Forest Science*, *72*(5), 595–607. https://doi.org/10.1007/s13595-015-0480-y

586 Allen, C. D., Macalady, A. K., Chenchouni, H., Bachelet, D., McDowell, N., Vennetier, M., … Cobb, N. (2010). A global

587   overview of drought and heat-induced tree mortality reveals emerging climate change risks for forests. *Forest Ecology*

588   *and Management*, *259*(4), 660–684. https://doi.org/10.1016/j.foreco.2009.09.001

589 Ameztegui, A., Cabon, A., De Cáceres, M., & Coll, L. (2017). Managing stand density to enhance the adaptability of Scots

590   pine stands to climate change: A modelling approach. *Ecological Modelling*, *356*.

591   https://doi.org/10.1016/j.ecolmodel.2017.04.006

592 Balducci, L., Deslauriers, A., Rossi, S., & Giovannelli, A. (2019). Stem cycle analyses help decipher the nonlinear response of

593   trees to concurrent warming and drought. *Annals of Forest Science*, *76*(3), 1–18. https://doi.org/10.1007/s13595-019-

594   0870-7

595 Baquedano, F J, & Castillo, F. J. (2007). Drought tolerance in the Mediterranean species Quercus coccifera , Quercus ilex ,

596   Pinus halepensis , and Juniperus phoenicea. *Photosynthetica*, *45*(2), 229–238.

597 Baquedano, Francisco J., Valladares, F., & Castillo, F. J. (2008). Phenotypic plasticity blurs ecotypic divergence in the response

598   of Quercus coccifera and Pinus halepensis to water stress. *European Journal of Forest Research*, *127*(6), 495–506.

599   https://doi.org/10.1007/s10342-008-0232-8

600 Barbeta, A., Mejia-Chang, M., Ogaya, R., Voltas, J., Dawson, T. E., & Peñuelas, J. (2015). The combined effects of a long-

601   term experimental drought and an extreme drought on the use of plant-water sources in a Mediterranean forest. *Global*

602   *Change Biology*, *21*, 1213–1225. https://doi.org/10.1111/gcb.12785

603 Barbeta, A., Ogaya, R., & Peñuelas, J. (2013). Dampening effects of long-term experimental drought on growth and mortality

604   rates of a Holm oak forest. *Global Change Biology*, *19*, 3133–3144. https://doi.org/10.1111/gcb.12269

605 Barton, K. (2018). MuMIn: Multi-Model Inference. R package version 1.42.1. Retrieved from https://cran.r-

606   project.org/package=MuMIn

607 Bello, J., Vallet, P., Perot, T., Balandier, P., Seigner, V., Perret, S., … Korboulewsky, N. (2019). How do mixing tree species

608   and stand density affect seasonal radial growth during drought events? *Forest Ecology and Management*, *432*(April

609   2018), 436–445. https://doi.org/10.1016/j.foreco.2018.09.044

610 Biging, G. S., & Dobbertin, M. (1995). Evaluation of Competition Indices in Individual Tree Growth Models. *Forest Science*,

611   *41*(2), 360–377.

612 Biondi, F., & Qeadan, F. (2008). A Theory-Driven Approach to Tree-Ring Standardization: Defining the Biological Trend

613   from Expected Basal Area Increment. *Tree-Ring Research*, *64*(2), 81–96. https://doi.org/10.3959/2008-6.1

614 Borghetti, M., Cinnirella, S., Magnani, F., & Saracino, A. (1998). Impact of long-term drought on xylem embolism and growth

615   in Pinus halepensis Mill. *Trees*, *12*(4), 187–195. https://doi.org/10.1007/s004680050139

616 Bréda, N., Granier, A., & Aussenac, G. (1995). Effects of thinning on soil and tree water relations, transpiration and growth in
617 an oak forest (Quercus petraea (Matt.) Liebl.). *Tree Physiology*, *15*(5), 295–306.
618 https://doi.org/10.1093/treephys/15.5.295

619 Calama, R., Conde, M., Madrigal, G., Vázquez-piqué, J., Javier, F., & Pardos, M. (2019). Linking climate , annual growth and
620 competition in a Mediterranean forest : Pinus pinea in the Spanish Northern Plateau. *Agricultural and Forest*
621 *Meteorology*, *264*(April 2018), 309–321. https://doi.org/10.1016/j.agrformet.2018.10.017

622 Calev, A., Zoref, C., Tzukerman, M., Moshe, Y., Zangy, E., & Osem, Y. (2016). High-intensity thinning treatments in mature
623 Pinus halepensis plantations experiencing prolonged drought. *European Journal of Forest Research*, *135*(3), 551–563.
624 https://doi.org/10.1007/s10342-016-0954-y

625 Campelo, F., Nabais, C., Freitas, H., & Gutiérrez, E. (2007). Climatic significance of tree-ring width and intra-annual density
626 fluctuations in *Pinus pinea* from a dry Mediterranean area in Portugal. *Annals of Forest Science*, *64*(2), 229–238.
627 https://doi.org/10.1051/forest:2006107

628 Canty, A., & Ripley, B. (2019). boot: Bootstrap R (S-Plus) Functions. R package version 1.3-22.

629 Carnicer, J., Coll, M., Ninyerola, M., Pons, X., Sánchez, G., & Peñuelas, J. (2011). Widespread crown condition decline, food
630 web disruption, and amplified tree mortality with increased climate change-type drought. *Proceedings of the National*
631 *Academy of Sciences of the United States of America*, *108*(4), 1474–1478. https://doi.org/10.1073/pnas.1010070108

632 Castagneri, D., Nola, P., Cherubini, P., & Motta, R. (2012). Temporal variability of size – growth relationships in a Norway
633 spruce forest : the influences of stand structure , logging , and climate. *Canadian Journal of Forest Research*, *42*, 550–
634 560. https://doi.org/10.1139/X2012-007

635 Cattaneo, N., Bravo, A., & Bravo, F. (2018). Analysis of tree interactions in a mixed Mediterranean pine stand using
636 competition indices. *European Journal of Forest Research*, *40*, 370–384. https://doi.org/10.1007/s10342-017-1094-8

637 Choat, B., Brodribb, T. J., Brodersen, C. R., Duursma, R. A., López, R., & Medlyn, B. E. (2018). Triggers of tree mortality
638 under drought and forest mortality. *Nature*, *558*, 531–539. https://doi.org/10.1038/s41586-018-0240-x

639 Condés, S., & García-Robredo, F. (2012). An empirical mixed model to quantify climate influence on the growth of Pinus
640 halepensis Mill . stands in South-Eastern Spain. *Forest Ecology and Management*, *284*, 59–68.
641 https://doi.org/10.1016/j.foreco.2012.07.030

642 Connell, J. H. (1990). Apparent versus "real" competition in plants. In J. . Grace & D. Tilman (Eds.), *Perspectives on Plant*
643 *Competition* (pp. 9–26). San Diego (California): Academic Press, Inc. https://doi.org/10.1016/b978-0-12-294452-
644 9.50006-0

645 Contreras, M. A., Affleck, D., & Chung, W. (2011). Evaluating tree competition indices as predictors of basal area increment
646 in western Montana forests. *Forest Ecology and Management*, *262*(11), 1939–1949.
647 https://doi.org/10.1016/j.foreco.2011.08.031

648 Cramer, W., Guiot, J., Fader, M., Garrabou, J., Gattuso, J.-P., Iglesias, A., … Xoplaki, E. (2018). Climate change and
649 interconnected risks to sustainable development in the Mediterranean. *Nature Climate Change*.

650	https://doi.org/10.1038/s41558-018-0299-2

651	Davison, A. C., & Hinkley, D. V. (1997). *Bootstrap Methods and Their Applications*. Cambridge: Cambridge University Press.

652	de Luis, M., Cufar, K., Filippo, A. Di, Novak, K., Papadopoulos, A., Piovesan, G., … Smith, K. T. (2013). Plasticity in

653	Dendroclimatic Response across the Distribution Range of Aleppo Pine (Pinus halepensis). *PLoS ONE*, *8*(12).

654	https://doi.org/10.1371/journal.pone.0083550

655	Dinno, A. (2017). dunn.test: Dunn's Test of Multiple Comparisons Using Rank Sums. R package version 1.3.5. Retrieved from

656	https://cran.r-project.org/package=dunn.test

657	Ettl, G. J., & Peterson, D. L. (1995). Extreme climate and variation in tree growth: individualistic response in subalpine fir

658	(Abies lasiocarpa). *Global Change Biology*, *1*(3), 231–241. https://doi.org/10.1111/j.1365-2486.1995.tb00024.x

659	Fatichi, S., Leuzinger, S., & Körner, C. (2013). Moving beyond photosynthesis : from carbon source to sink-driven vegetation

660	modeling. *New Phytologist*, (201), 1086–1095.

661	Forner, A., Valladares, F., Bonal, D., Granier, A., Grossiord, C., & Aranda, I. (2018). Extreme droughts affecting

662	Mediterranean tree species ' growth and water-use efficiency : the importance of timing. *Tree Physiology*, (March), 1–

663	11. https://doi.org/10.1093/treephys/tpy022

664	Fox, J., & Weisberg, S. (2018a). *An R companion to Applied Regression*. (T. Oaks, Ed.) (3rd Editio). CA.

665	Fox, J., & Weisberg, S. (2018b). Defining Effect Methods for Other Models Using effects with Other Modeling Methods , with

666	Generalized Least Squares in the nlme package as an Example, 1–14.

667	Froux, F., Ducrey, M., & Dreyer, E. (2005). Vulnerability to embolism differs in roots and shoots and among three

668	Mediterranean conifers : consequences for stomatal regulation of water loss ? *Trees*, *19*, 137–144.

669	https://doi.org/10.1007/s00468-004-0372-5

670	Gazol, A., Camarero, J. J., Vicente-Serrano, S. M., Sánchez-Salguero, R., Gutiérrez, E., de Luis, M., … Galván, J. D. (2018).

671	Forest resilience to drought varies across biomes. *Global Change Biology*, *24*(5), 2143–2158.

672	https://doi.org/10.1111/gcb.14082

673	Giorgi, F. (2006). Climate change hot-spots. *Geophysical Research Letters*, *33*(8), 1–4. https://doi.org/10.1029/2006GL025734

674	Granier, A., Bréda, N., Biron, P., & Villette, S. (1999). A lumped water balance model to evaluate duration and intensity of

675	drought constraints in forest stands. *Ecological Modeling*, *116*, 269–283. Retrieved from file:///C:%5CDocuments and

676	Settings%5COliver%5CMes documents%5CMyPDFs%5C1999%5CGranier.1999.pdf

677	Granier, A., Reichstein, M., Bréda, N., Janssens, I. A., Falge, E., Ciais, P., … Wang, Q. (2007). Evidence for soil water control

678	on carbon and water dynamics in European forests during the extremely dry year : 2003. *Agricultural and Forest*

679	*Meteorology*, *143*(May 2006), 123–145. https://doi.org/10.1016/j.agrformet.2006.12.004

680	Greenwood, S., Ruiz-Benito, P., Martínez-Vilalta, J., Lloret, F., Kitzberger, T., Allen, C. D., … Jump, A. S. (2017). Tree

681	mortality across biomes is promoted by drought intensity, lower wood density and higher specific leaf area. *Ecology*

682	*Letters*, *20*(4), 539–553. https://doi.org/10.1111/ele.12748

683	Hayles, L. A., Gutierrez, E., Macias, M., Ribas, M., Bosch, O., & Camarero, J. J. (2007). Climate increases regional tree-

growth variability in Iberian pine forests. *Global Change Biology*, *13*(7), 804–815. https://doi.org/10.1111/j.1365-2486.2007.01322.x

Hover, A., Buissart, F., Caraglio, Y., Heinz, C., Pailler, F., Ramel, M., … Sabatier, S. (2017). Growth phenology in Pinus halepensis Mill.: apical shoot bud content and shoot elongation. *Annals of Forest Science*, *74*(2), 39. https://doi.org/10.1007/s13595-017-0637-y

Hsiao, T. C., Acevedo, E., Fereres, E., & Henderson, D. W. (1976). Water Stress, Growth, and Osmotic Adjustment. *Phil. Trans. R. Soc. Lond. B*, *273*(February), 479–500. https://doi.org/10.1098/rstb.1976.0026

IPCC. (2014). *Climate Change 2014: Synthesis Report. Contribution of Working Groups I, II, III to the Fifth Assessment Report of the Intergovernmental Panel on Climate Change*. Geneva, Switzerland. https://doi.org/10.1177/0002716295541001010

Jabiol, B., Lévy, G., Bonneau, M., & Brêthes, A. (2009). *Comprendre les sols pour mieux gérer les forêts. AgroParisTech*. Nancy: AgroParisTech.

Klein, T., Cohen, S., & Yakir, D. (2011). Hydraulic adjustments underlying drought resistance of Pinus halepensis. *Tree Physiology*, *31*, 637–648. https://doi.org/10.1093/treephys/tpr047

Kuznetsova, A., Brockhoff, P., & Christensen, R. (2017). lmerTest Package: Tests in Linear Mixed Effects Models. *Journal of Statistical Software*, *82*(13), 1–26.

Lebourgeois, F., Eberlé, P., Mérian, P., & Seynave, I. (2014). Social status-mediated tree-ring responses to climate of Abies alba and Fagus sylvatica shift in importance with increasing stand basal area. *Forest Ecology and Management*, *328*, 209–218. https://doi.org/10.1016/j.foreco.2014.05.038

Lempereur, M., Martin-stpaul, N. K., Damesin, C., Joffre, R., Ourcival, J., Rocheteau, A., & Rambal, S. (2015). Growth duration is a better predictor of stem increment than carbon supply in a Mediterranean oak forest : implications for assessing forest productivity under climate change. *New Phytologist*.

Liu, X., Sun, G., Mitra, B., Noormets, A., Gavazzi, M. J., Domec, J. C., … McNulty, S. G. (2018). Drought and thinning have limited impacts on evapotranspiration in a managed pine plantation on the southeastern United States coastal plain. *Agricultural and Forest Meteorology*, *262*(June), 14–23. https://doi.org/10.1016/j.agrformet.2018.06.025

Martin-Benito, D., Kint, V., Muys, B., & Cañellas, I. (2011). Growth responses of West-Mediterranean Pinus nigra to climate change are modulated by competition and productivity : Past trends and future perspectives. *Forest Ecology and Management*, *262*(6), 1030–1040. https://doi.org/10.1016/j.foreco.2011.05.038

Maseyk, K. S., Lin, T., Rosenberg, E., Grünzweig, J. M., Schwartz, A., & Yakir, D. (2008). Physiology – phenology interactions in a productive semi-arid pine forest. *New Phytologist*, *178*, 603–616.

McCullagh, P. (2000). Resampling and Exchangeable Arrays. *Bernoulli*, *6*(2), 285–301. https://doi.org/10.2307/3318577

Melzack, R. N., Bravdo, B., & Riov, J. (1985). The effect of water stress on photosynthesis and related parameters in Pinus halepensis, (February), 295–300.

Millar, C. I., Stephenson, N. L., & Stephens, S. L. (2007). Climate change and forest of the future: Managing in the face of

718 uncertainty. *Ecological Applications*, *17*(8), 2145–2151. https://doi.org/http://dx.doi.org/10.1890/06-1715.1

719 Mina, M., Martin-Benito, D., Bugmann, H., & Cailleret, M. (2016). Forward modeling of tree-ring width improves simulation

720 of forest growth responses to drought. *Agricultural and Forest Meteorology*, *221*, 13–33.

721 https://doi.org/10.1016/j.agrformet.2016.02.005

722 Misson, L., Rathgeber, C., & Guiot, J. (2004). Dendroecological analysis of climatic effects on *Quercus petraea* and *Pinus*

723 *halepensis* radial growth using the process-based MAIDEN model. *Canadian Journal of Forest Research*, *34*(4), 888–

724 898. https://doi.org/10.1139/x03-253

725 Molina, A. J., & del Campo, A. D. (2012). The effects of experimental thinning on throughfall and stemflow: A contribution

726 towards hydrology-oriented silviculture in Aleppo pine plantations. *Forest Ecology and Management*, *269*, 206–213.

727 https://doi.org/10.1016/j.foreco.2011.12.037

728 Muller, B., Pantin, F., Génard, M., Turc, O., Freixes, S., Piques, M., & Gibon, Y. (2011). Water deficits uncouple growth from

729 photosynthesis , increase C content , and modify the relationships between C and growth in sink organs. *Journal of*

730 *Experimental Botany*, *62*(6), 1715–1729. https://doi.org/10.1093/jxb/erq438

731 Norman, J. M., & Jarvis, P. G. (1975). Photosynthesis in Sitka Spruce (Picea sitchensis (Bong.) Carr): V. Radiation Theory

732 and a Test case. *Journal of Applied Ecology*, *12*(3), 839–878.

733 Novick, K. A., Ficklin, D. L., Stoy, P. C., Williams, C. A., Bohrer, G., Oishi, A. C., … Phillips, R. P. (2016). The increasing

734 importance of atmospheric demand for ecosystem water and carbon fluxes. *Nature Climate Change*, *6*(11), 1023–1027.

735 https://doi.org/10.1038/nclimate3114

736 Ogaya, R., Peñuelas, J., Martínez-Vilalta, J., & Mangirón, M. (2003). Effect of drought on diameter increment of Quercus ilex,

737 Phillyrea latifolia, and Arbutus unedo in a holm oak forest of NE Spain. *Forest Ecology and Management*, *180*(1–3),

738 175–184. https://doi.org/10.1016/S0378-1127(02)00598-4

739 Olivar, J., Bogino, S., Rathgeber, C., Bonnesoeur, V., & Bravo, F. (2014). Thinning has a positive effect on growth dynamics

740 and growth-climate relationships in Aleppo pine (Pinus halepensis) trees of different crown classes. *Annals of Forest*

741 *Science*, *71*(3), 395–404. https://doi.org/10.1007/s13595-013-0348-y

742 Olivar, J., Bogino, S., Spiecker, H., & Bravo, F. (2012). Climate impact on growth dynamic and intra-annual density

743 fluctuations in Aleppo pine (Pinus halepensis) trees of different crown classes. *Dendrochronologia*, *30*(1), 35–47.

744 https://doi.org/10.1016/j.dendro.2011.06.001

745 Pasho, E., Camarero, J. J., & Vicente-Serrano, S. M. (2012). Climatic impacts and drought control of radial growth and seasonal

746 wood formation in Pinus halepensis. *Trees*, 1875–1886. https://doi.org/10.1007/s00468-012-0756-x

747 Peñuelas, J., Sardans, J., Filella, I., Estiarte, M., Llusià, J., Ogaya, R., … Terradas, J. (2017). Impacts of global change on

748 Mediterranean forests and their services. *Forests*, *8*(12), 1–37. https://doi.org/10.3390/f8120463

749 Pretzsch, H., & Biber, P. (2010). Size-symmetric versus size-asymmetric competition and growth partitioning among trees in

750 forest stands along an ecological gradient in central Europe. *Canadian Journal of Forest Research*, *384*, 370–384.
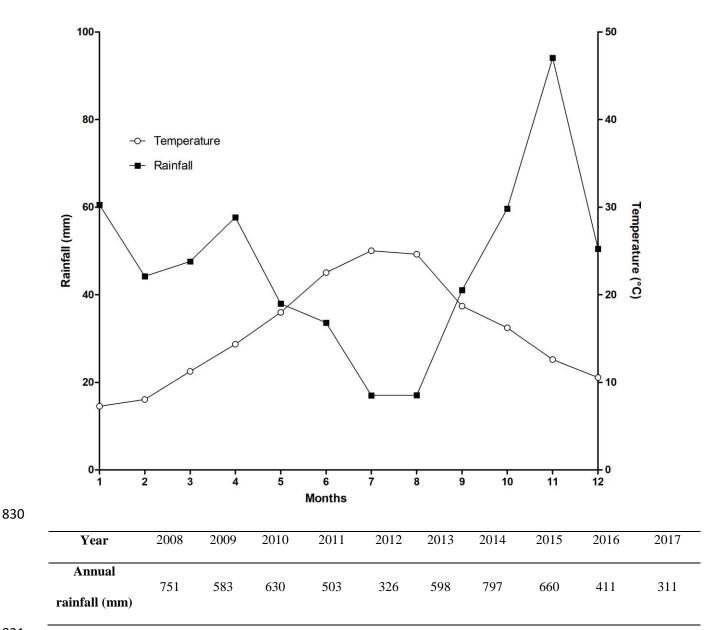
751 https://doi.org/10.1139/X09-195

752 Pretzsch, H., Forrester, D. I., & Bauhus, J. (2017). *Mixed-species forests. Ecology and management*. (H. Pretzsch, D. I.

753   Forrester, & J. Bauhus, Eds.). Berlin: Springer.

754 Prévosto, B. (2005). Outils et Méthodes : les indices de compétition en foresterie : exemples d'utilisation, intérêts et limites.

755   *Revue Forestière Française*, *LVII*(5), 413–430.

756 Prévosto, B., Audouard, M., Helluy, M., Lopez, J.-M., & Balandier, P. (2018). *Le bilan hydrique en forêt méditerranéenne :*

757   *influence des strates et de leur gestion Application au pin d'Alep*. *Forêt Méditerranéenne* (Vol. XXXIX). Retrieved

758   from https://appgeodb.

759 Prévosto, B., Helluy, M., Gavinet, J., Fernandez, C., & Balandier, P. (2019). Microclimate and Mediterranean pine forests:

760   What is the influence of the shrub layer? *Agricultural and Forest Meteorology*, (in press). https://doi.org/doi :

761   10.1016/j.agrformet.2019.107856

762 Pukkala, T., & Kolström, T. (1987). Competition indices and the prediction of radial growth in Scots pine. *Silva Fennica*.

763   https://doi.org/10.14214/sf.a15463

764 R Core Team. (2017). R: A language and environment for statistical computing. Vienna, Austria: R Foundation for Statistical

765   Computing.

766 Rathgeber, C. B. K., Misson, L., Nicault, A., & Guiot, J. (2005). Bioclimatic model of tree radial growth : application to the

767   French Mediterranean Aleppo pine forests. *Trees*, 162–176. https://doi.org/10.1007/s00468-004-0378-z

768 Rouvinen, S., & Kuuluvainen, T. (1997). Structure and asymmetry of tree crowns in relation to local competition in a natural

769   mature Scots pine forest. *Canadian Journal of Forest Research*, *27*(6), 890–902. https://doi.org/10.1139/x97-012

770 Sánchez-Salguero, R., Linares, J. C., Camarero, J. J., Madrigal-González, J., Hevia, A., Sánchez-Miranda, Á., … Rigling, A.

771   (2015). Disentangling the effects of competition and climate on individual tree growth: A retrospective and dynamic

772   approach in Scots pine. *Forest Ecology and Management*, *358*, 12–25. https://doi.org/10.1016/j.foreco.2015.08.034

773 Sanginés de Cárcer, P., Vitasse, Y., Peñuelas, J., Jassey, V. E. J., Buttler, A., & Signarbieux, C. (2018). Vapor–pressure deficit

774   and extreme climatic variables limit tree growth. *Global Change Biology*, *24*(3), 1108–1122.

775   https://doi.org/10.1111/gcb.13973

776 Schröder, J., & Gadow, K. Von. (1999). Testing a new competition index for Maritime pine in northwestern Spain. *Canadian*

777   *Journal of Forest Research*, *283*(Table 1), 280–283.

778 Schwinning, S., & Weiner, J. (1998). Mechanisms determining the degree of size asymmetry in competition among plants.

779   *Oecologia*, *113*(4), 447–455. https://doi.org/10.1007/s004420050397

780 Signorell, A., & al., et mult. (2019). DescTools: Tools for descriptive statistics. *R Package Version 0.99.27*. Retrieved from

781   https://cran.r-project.org/package=DescTools

782 Simonin, K., Kolb, T. E., Montes-Helu, M., & Koch, G. W. (2007). The influence of thinning on components of stand water

783   balance in a ponderosa pine forest stand during and after extreme drought. *Agricultural and Forest Meteorology*, *143*(3–

784   4), 266–276. https://doi.org/10.1016/j.agrformet.2007.01.003

785 Sohn, J. A., Saha, S., & Bauhus, J. (2016). Potential of forest thinning to mitigate drought stress: A meta-analysis. *Forest*

786   *Ecology and Management*, *380*, 261–273. https://doi.org/10.1016/j.foreco.2016.07.046

787   Soto, A., Robledo-Arnuncio, J. J., González-Martínez, S. C., Smouse, P. E., & Alía Miranda, R. (2010). Climatic niche and

788   neutral genetic diversity of the six Iberian pine species: A retrospective and prospective view. *Molecular Ecology*, *19*(7),

789   1396–1409. https://doi.org/10.1111/j.1365-294X.2010.04571.x

790   Speich, M. J. R. (2019). Quantifying and modeling water availability in temperate forests: A review of drought and aridity

791   indices. *IForest Biogeoscience and Forestry*, *12*(1), 1–16. https://doi.org/10.3832/ifor2934-011

792   Tardieu, F., Granier, C., & Muller, B. (2011). Water deficit and growth. Co-ordinating processes without an orchestrator?

793   *Current Opinion in Plant Biology*, *14*, 283–289. https://doi.org/10.1016/j.pbi.2011.02.002

794   Trouvé, R., Bontemps, J. D., Collet, C., Seynave, I., & Lebourgeois, F. (2017). Radial growth resilience of sessile oak after

795   drought is affected by site water status, stand density, and social status. *Trees - Structure and Function*, *31*(2), 517–529.

796   https://doi.org/10.1007/s00468-016-1479-1

797   Turc, L. (1961). Évalutation des besoins en eau d'irrigation, évapotranspiration potentielle. *Ann. Agron.*, *12*(1), 13–49.

798   Ungar, E. D., Rotenberg, E., Raz-Yaseef, N., Cohen, S., Yakir, D., & Schiller, G. (2013). Transpiration and annual water

799   balance of Aleppo pine in a semiarid region: Implications for forest management. *Forest Ecology and Management*,

800   *298*, 39–51. https://doi.org/10.1016/j.foreco.2013.03.003

801   Vennetier, M., Ripert, C., & Rathgeber, C. (2018). Autecology and growth of Aleppo pine (Pinus halepensis Mill.): A

802   comprehensive study in France. *Forest Ecology and Management*, *413*(November 2017), 32–47.

803   https://doi.org/10.1016/j.foreco.2018.01.028

804   Vilà-Cabrera, A., Coll, L., Martínez-Vilalta, J., & Retana, J. (2018). Forest management for adaptation to climate change in

805   the Mediterranean basin: A synthesis of evidence. *Forest Ecology and Management*, *407*(August 2017), 16–22.

806   https://doi.org/10.1016/j.foreco.2017.10.021

807   Vizcaíno-Palomar, N., Ibáñez, I., González-Martínez, S. C., Zavala, M. A., & Alía, R. (2016). Adaptation and plasticity in

808   aboveground allometry variation of four pine species along environmental gradients. *Ecology and Evolution*, *6*(21),

809   7561–7573. https://doi.org/10.1002/ece3.2153

810   Voltas, J., Lucabaugh, D., Chambel, M. R., & Ferrio, J. P. (2015). Intraspecific variation in the use of water sources by the

811   circum-Mediterranean conifer Pinus halepensis. *New Phytologist*, *208*(4), 1031–1041.

812   https://doi.org/10.1111/nph.13569

813   Voltas, J., Shestakova, T. A., Patsiou, T., di Matteo, G., & Klein, T. (2018). Ecotypic variation and stability in growth

814   performance of the thermophilic conifer Pinus halepensis across the Mediterranean basin. *Forest Ecology and*

815   *Management*, *424*(March), 205–215. https://doi.org/10.1016/j.foreco.2018.04.058

816   Weiskittel, A. R., Hann, D. W., Kershaw Jr, J. A., & Vanclay, J. K. (2011). *Forest Growth and Yield Modeling*. (J. W. & Sons,

817   Ed.).

818   Wykoff, W. R., Crookston, N. L., & Stage, A. R. (1982). *User's Guide to the Stand Prognosis Model General Technical Report*
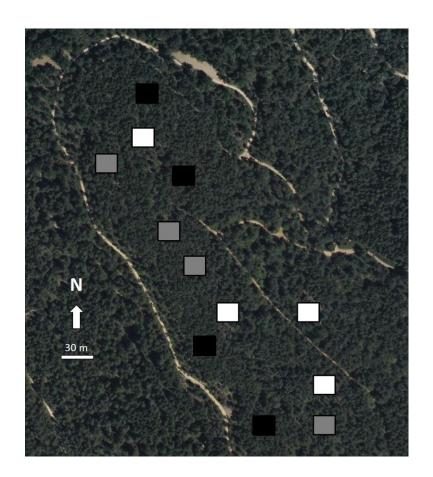
819   *INT-122*.

820 Zang, C., Pretzsch, H., & Rothe, A. (2012). Size-dependent responses to summer drought in Scots pine , Norway spruce and

821 common oak. *Trees*, *26*, 557–569. https://doi.org/10.1007/s00468-011-0617-z

822 Zweifel, R., Zimmermann, L., Zeugin, F., & Newbery, D. M. (2006). Intra-annual radial growth and water relations of trees:

823 Implications towards a growth mechanism. *Journal of Experimental Botany*, *57*(6), 1445–1459.

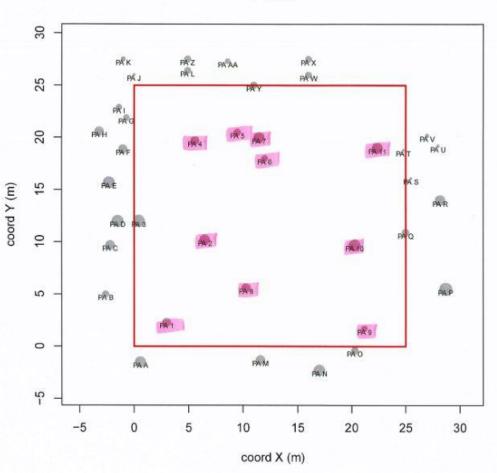824 https://doi.org/10.1093/jxb/erj125

825

826 **SUPPLEMENTARY MATERIAL**

827 **Appendix A: Ombrothermic diagram based on records from the study period (Istres weather station, 2008-**

828 **2017).** Below the figure are some additionnal data concerning annual rainfall.

829

830

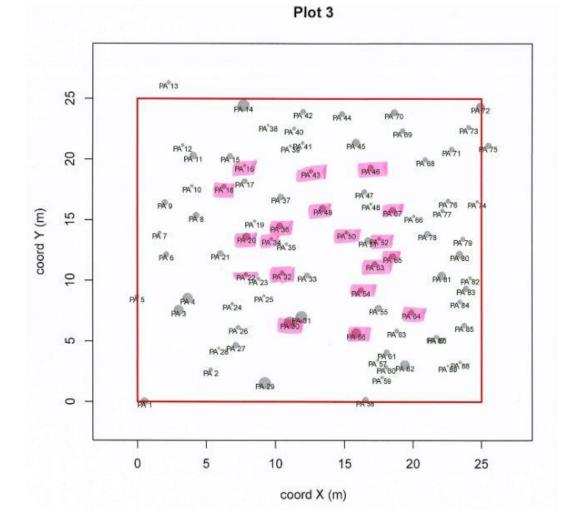| Year	2008	2009	2010	2011	2012	2013	2014	2015	2016	2017
Annual rainfall (mm)	751	583	630	503	326	598	797	660	411	311

831

832   **Appendix B: Location of the 12 plots used in the study.** Treatments are, as follow: dense cover (black squares),

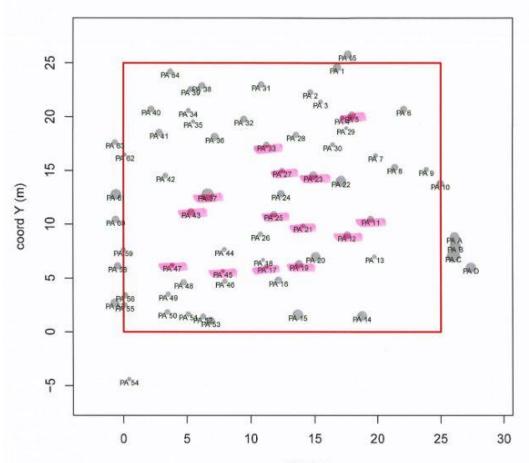833   medium cover (grey squares) and light cover (white squares).

834

835

836

837

838

839

840

841

842

843

844

845

846

847

848

849 **Appendix C: Location of the selected trees for the dendroecological analysis.** "Plot 2" is from the light cover

850 treatment, "Plot 3" is from the dense cover treatments, "Plot" 9 is from the medium cover treatment. The dots

851 represent the trees, the size of a dot represent the size (circumference) of the trees. The highlighted dots are the

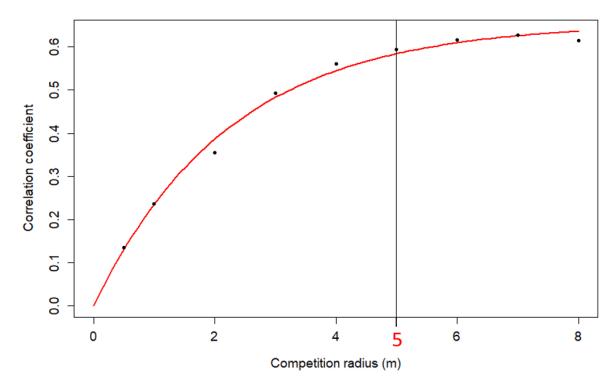852 trees that were selected for the analysis.

853

Plot 3

854

Plot 9

855
856
857
858
859
860
861
862
863
864
865
866
867
868

869   **Appendix D: Selection of the competition radius**. The correlation coefficient is the mean BAI for 10 years

870   divided by a competition index (for example here it is Hegyi competition index) according to the competition

871   radius used for the computation of the competition index. Curve fit: Correlation coefficient = 0,654606 * (1 - exp(-

872   0,445734 * competition radius)). We chose a competition radius of 5 meters, as the correlation coefficient only

873   slightly increased after 5 meters (asymptote at y = 7), and because of the sampling design (the trees that were cored

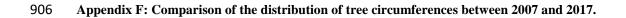874   were selected in the 20m*20m inner plot and the inventories were done in a 25 m * 25 m area).

875

876

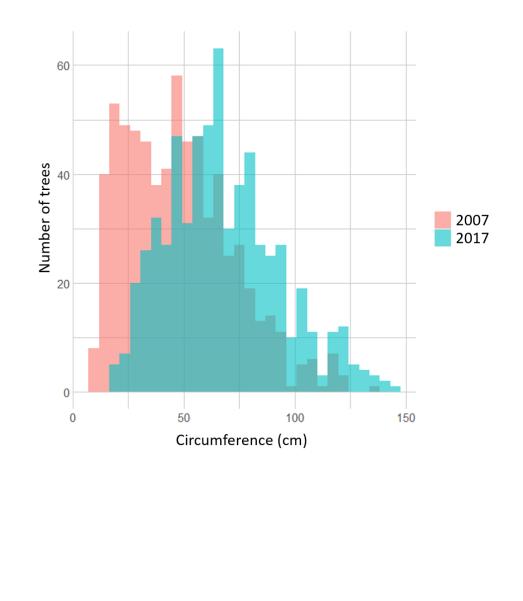877

878

879

880

881

882

883

884

885 **Appendix E: Results from the models tested during the preliminary analysis**. Linear mixed-effects models of

886 the annual tree basal area increment (BAI) as a function of the basal area of the previous year (BA) and the different

887 indices, both annual and seasonal. *BAL* is the BAL CI, taken here as an example. The annual WSIs are the rainfall,

888 the maximum temperature (max T), the minimum temperature (min T), the average temperature (avg T), and *INT*

889 taken here as an example of the WSIs retained for the final analyses. The seasonal WSI are ordered according to

890 the season (winter, spring, summer and autumn). The best models according to AIC are in bold.

Models (with tree as random effect on the intercept)	Marg. R^2	Cond. R^2	AIC
log(BAI) ~ log(BA) + log(IC$_5$) + log(*INT*)	**0.48**	**0.77**	**2735.3**
log(BAI) ~ log(BA) + log(IC$_5$) + log(Rainfall)	**0.34**	**0.87**	**2767.7**
log(BAI) ~ log(BA) + log(*INT*)	**0.43**	**0.72**	**2795.8**
log(BAI) ~ log(*INT*)	**0.16**	**0.77**	**2831.9**
log(BAI) ~ log(BA) + log(Rainfall)	**0.12**	**0.88**	**2885.3**
log(BAI) ~ log(Rainfall)	**0.10**	**0.79**	**2893.8**
log(BAI) ~ log(BA) + log(IC$_5$) + log(autumn *INT*)	0.34	0.86	2900.3
log(BAI) ~ log(BA) + log(IC$_5$) + log(winter Rainfall)	0.33	0.90	2949.6
log(BAI) ~ log(BA) + log(IC$_5$) + log(summer Rainfall)	0.34	0.92	2969.3
log(BAI) ~ log(BA) + log(autumn *INT*)	0.15	0.90	3031.4
log(BAI) ~ log(autumn *INT*)	0.10	0.75	3052.8
log(BAI) ~ log(BA) + log(IC$_5$) + log(summer *INT*)	0.33	0.85	3059.5
log(BAI) ~ log(BA) + log(IC$_5$) + log(max T)	0.36	0.94	3076.3
log(BAI) ~ log(BA) + log(winter Rainfall)	0.22	0.94	3079.9
log(BAI) ~ log(BA) + log(summer Rainfall)	0.26	0.96	3103.2
log(BAI) ~ log(BA) + log(IC$_5$) + log(spring *INT*)	0.32	0.81	3154.8
log(BAI) ~ log(winter Rainfall)	0.07	0.75	3161.9
log(BAI) ~ log(BA) + log(summer *INT*)	0.12	0.86	3184.3
log(BAI) ~ log(summer *INT*)	0.09	0.72	3190.3
log(BAI) ~ log(BA) + log(IC$_5$) + log(autumn Rainfall)	0.31	0.85	3207.1
log(BAI) ~ log(BA) + log(max T)	0.30	0.97	3213.7
log(BAI) ~ log(BA) + log(IC$_5$) + log(min T)	0.35	0.93	3256.0
log(BAI) ~ log(BA) + log(spring *INT*)	0.20	0.62	3262.4

log(BAI) ~ log(summer Rainfall)	0.05	0.73	3263.2
log(BAI) ~ log(spring INT)	0.07	0.71	3264.5
log(BAI) ~ log(BA) + log(IC_5) + log(avg T)	0.32	0.90	3293.8
log(BAI) ~ log(BA) + log(IC_5) + log(winter INT)	0.32	0.90	3295.4
log(BAI) ~ log(BA) + log(IC_5) + log(spring Rainfall)	0.33	0.91	3303.3
log(BAI) ~ log(BA) + log(autumn Rainfall)	0.11	0.86	3329.8
log(BAI) ~ log(autumn Rainfall)	0.04	0.72	3334.4
log(BAI) ~ log(BA) + log(min T)	0.30	0.97	3393.2
log(BAI) ~ log(BA) + log(avg T)	0.24	0.94	3427.3
log(BAI) ~ log(BA) + log(winter INT)	0.24	0.94	3428.4
log(BAI) ~ log(BA) + log(spring Rainfall)	0.25	0.95	3437.5
log(BAI) ~ log(max T)	0.01	0.69	3491.4
log(BAI) ~ log(winter INT)	0.01	0.69	3514.7
log(BAI) ~ log(avg T)	0.01	0.69	3524.2
log(BAI) ~ log(spring Rainfall)	0.00	0.68	3554.1
log(BAI) ~ log(min T)	0.00	0.68	3568.6

891 *Abbreviations: Marg. R² the marginal r-squared (accounting for the fixed effects); Cond. R² the conditional r-squared*

892 *(accounting for the fixed and random effects); AIC the Akaike Information Criterion;*

893

894

895

896

897

898

899

900

901

902

903

904

905

Appendix F: Comparison of the distribution of tree circumferences between 2007 and 2017.

907

908

909

910

911

912

913

914

915

916

917

918

919

920

921 **Appendix G: Circumferences plotted against heights for all of the individuals used in the study.** These are

922 measurements taken from 2017.

923